THE AMERICAN SOCIETY OF MECHANICAL ENGINEERS
345 E. 47 St., New York, N.Y. 10017

The Society shall not be responsible for statements or opinions advanced in papers or in discussion at meetings of the Society or of its Divisions or Sections, or printed in its publications. Discussion is printed only if the paper is published in an ASME Journal. Released for general publication upon presentation. Full credit should be given to ASME, the Technical Division, and the author(s). Papers are available from ASME for nine months after the meeting.
Printed in USA.

Copyright © 1982 by ASME

82-GT-10

The Performance of Centrifugal Compressor Channel Diffusers

C. Rodgers
Turbomach,
A Division of Solar Turbines Inc.,
San Diego, CA

Test results pertaining to the characteristics of single-stage centrifugal compressors with backswept impellers and channel-type diffusers are presented and analyzed to formulate major performance criteria influencing maximum diffusion capability. For any given stage, it was determined that stage surge (when triggered by diffuser stall), occurred near a constant mean stream velocity diffusion ratio between the impeller tip and diffuser throat. This diffusion ratio attained a maximum value of 1.8 for impeller tip Mach numbers less than unity, but was not unique for all stages, being more intimately coupled with throat blockage accumulation as a function of diffusion rate. This was identified by testing some vaned diffusers beyond the stall limit where rapid blockage accumulation precipitated an immediate decrease in channel diffuser and system static pressure recovery. The results of various experiments in the vaneless space are also described to illustrate the sensitivity of the vaneless space flow upon centrifugal compressor performance.

NOMENCLATURE

A	Area
AS	Aspect Ratio (=b/w)
b	Vane Height
B	Blockage Factor
B_n	Normalized Blockage Factor
C_p	Static Pressure Recovery
C_D	Discharge Coefficient
C	Absolute Velocity
D	Diameter
i_3	Throat Incidence
L	Vane Length
N	Rotational Speed
P	Total Pressure
p	Static Pressure
q	Impeller Work Factor
T	Total Temperature
U	Impeller Tip Speed
W	Flow, Throat Width, Relative Velocity
Z	Vane Number
δ	Boundary Layer Displacement Thickness
α	Absolute Flow Angle
η	Efficiency

SUBSCRIPT

1	Impeller Inlet
2	Impeller Tip
3	Diffuser Throat
4	Diffuser Exit (covered)
E	Exit
R	Radial

SUPERSCRIPT

*	Unblocked Velocity

UNITS

The following units were used in evaluation of the compressor performance. Equivalent metric conversions are noted.

Item	English	Metric Conversion
Ns	rpm $(cfs)^{0.5}$ X $Had^{-0.75}$	1 rpm $(M^3/S)^{0.5}{}_m{}^{-0.75}$ = 0.412 X Ns
C; U; W	fps	1 m/s = 3.281 fps
D; L; r;t	in.	1 cm = 0.3937 in.
$\alpha 1$; $\alpha 2$	deg	---
ρ	lb/ft^3	$1 kg/m^3$ = 0.0625 lb/ft^3
cp	Btu/lb	1 J/kg = 0.43 X 10^{-3} Btu/lb
P;p	psia	1 kg/m^2 = 1.422 X 10^{-3} psia
T	deg R	deg K = deg R/1.8

Contributed by the Gas Turbine Division of the ASME.

Downloaded from http://asmedigitalcollection.asme.org/GT/proceedings-pdf/GT1982/79566/V001T01A003/2394014/v001t01a003-82-gt-10.pdf by guest on 21 August 2022

INTRODUCTION

Flow ranges for single-stage centrifugal compressors are dictated by the stalling characteristics of the impeller and the diffuser which are intrinsically controlled by the diffusion capability or attainable static pressure rise of the blade and vane rows. Although both vaned and vaneless diffuser systems are used for centrifugal compressors, the requirement for maximum efficiency at high Mach numbers makes the use of vaned diffuser systems almost mandatory. The impeller and diffuser must be matched simultaneously at their peak efficiency flow conditions.

The stationary vaned diffuser tends to be the flow controlling component in that its overall Mach number level and inlet blockage are higher than those of the inducer which operates with a large radial variation of Mach numbers from hub to shroud. The diffuser must also accept an already diffused flow from the impeller with resulting non-uniform entrance conditions which further aggravate its stalling sensitivity. These conditions curtail the compressor operating range and, as a result, stationary diffusers for centrifugal compressors have received considerable attention. Attainment of a large flow range requires that the impeller and the diffuser must be capable of extended operation into their stalled or positive incidence regions to a flow where static pressure rise plateaus, and compressor surge is eventually triggered. Stage surge is believed to stem from operation on an unstable (positive slope) portion of the overall compressor characteristic, where the static pressure ratio increases with increasing flow. One effective method of increasing compressor operating range is to provide sufficient impeller stability so that the downstream diffuser can operate slightly into its positive incidence zone, even though the diffuser static pressure recovery versus flow characteristic exhibits a positive slope.

Previous studies by the author on centrifugal impeller diffusion limitations were presented in Reference [1] and pertained to analysis of a single, experimental, high Mach number, centrifugal, backswept impeller of near optimum configuration. Test results on this particular impeller indicated impeller stalling occurred whenever the relative velocity diffusion ratio, W_{IRMS}/W_2, (based on mixed impeller exit condition) exceeded 1.6. It was, therefore, suggested that such a simple limiting velocity ratio could be used as an initial design guideline to indicate impeller stalling proximity. The informative discussion in Reference [1] added a precautionary tone in that application of such a simple stalling proposition to all centrifugal impeller designs might be premature. Bearing this precaution in mind, additional research was conducted on the stalling characteristics of a wide variety of centrifugal impeller designs, mostly of the inducer type with back-sweep angles of 40-45 degrees, relative to the radial direction).

The goals in conducting this additional research were continued improvement in performance levels, performance prediction techniques, and, particularly, the identification of key factors improving stable operating flow range of both the impeller and diffuser. Analysis of the impeller performances suggested that a modified diffusion factor, including the effects of meridional curvature and blade solidity, provided improved

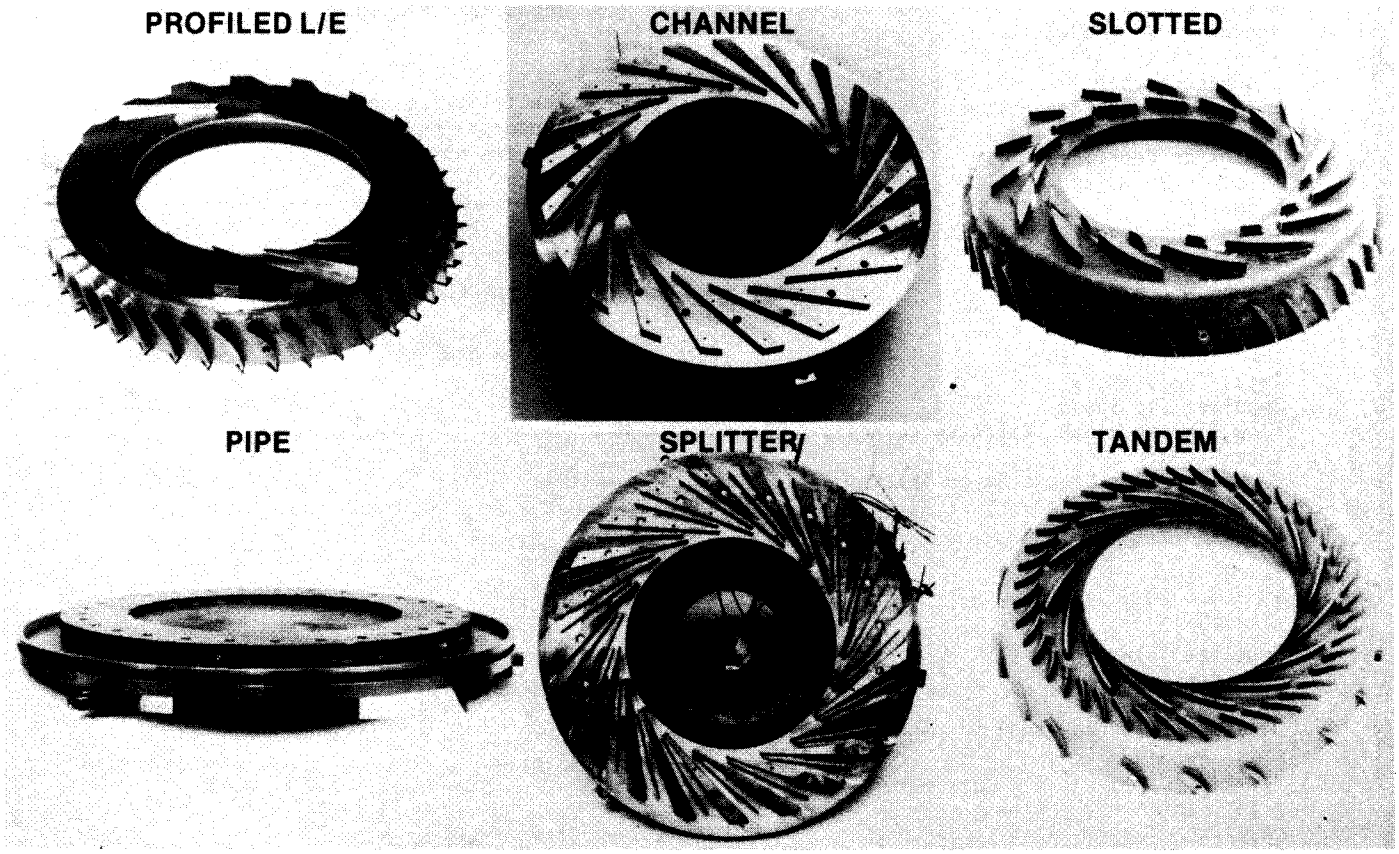

Fig. 1 Types of centrifugal compressor diffusers

Downloaded from http://asmedigitalcollection.asme.org/GT/proceedings-pdf/GT1982/79566/V001T01A003/2394014/v001t01a003-82-gt-10.pdf by guest on 21 August 2022

stall correlation for a wide specific speed range of impeller types.

Extensive compressor component performance data was obtained for the tests and apparatus described in Reference [2]. Single stage testing was accomplished with both vaneless parallel wall diffusers downstream of each impeller and vaned channel diffusers. Subsequent analysis of both the vaneless and vaned diffuser configurations tested has led to a further understanding of the stator static diffusion process which is the subject of this paper.

REVIEW OF DIFFUSER TECHNOLOGY

High performance centrifugal compressors require the use of an efficient diffusion system at the impeller exit capable of converting the kinetic energy leaving the impeller into the maximum static pressure recovery over a wide range of incident flow conditions. Many types of diffusion systems have been studied, including two-dimensional channel diffusers, conical pipe diffusers, cascade diffusers, rotating diffusers, and vaneless diffusers (See References [1] through [11]). Some of the diffusion systems investigated by the author are shown in Figure 1, and encompass diffusion in both the radial plane and radial plus axial planes. This paper addresses the subject of diffusion in the radial plane only, since the critical initial entry section in the radial plane between the impeller tip and diffuser throat plays a dominant role in dictating compressor performance.

Complex compound large area ratio diffusers with integral tail pipes, Reference [3], can be used to obtain quite low exit velocities and, therefore, high static pressure recoveries. Such diffuser systems are inclined to be costly in both development and manufacture and cannot be readily resized to provide a family of diffusers for varying flow capacity.

Diffusion limitations for centrifugal compressors are discussed in References [4] through [7]. Rundstadler demonstrated that the single most important parameter governing the channel diffuser recovery is the boundary layer blockage at the throat. This is particularly unfortunate to the compressor performance prediction analyst since the blockage is partially controlled by the complex impeller discharge flow and mixing process. Analytical blockage determination is, therefore, questionable, and reversion to empirical correlation is often the recourse. Reference [5] pointed out the conflict between the requirements for increased flow range and efficiency in selection of the vaneless space geometry. Blockage grows in the vaneless space, but Mach number reduces. The recommendation was in favor of the short vaneless space if the vaned diffuser could be designed for efficient entry transonic diffusion.

In Reference [6] different vaned diffusers were tested in a compressor rig. These test results showed that the pressure recovery increased up to a critical diffusion limit which was approximately 2.0 (defined as C_4/C_2).

A clearer picture of the murky diffuser entry flow field has been obtained with advanced laser velocimeter equipment. Krain, Reference [7], made detailed optical measurements within the diffuser entry section showing evidence of periodically fluctuating highly distorted flow. Comparative measurements within the impeller discharge region for both the vaneless and vaned diffuser designs tested revealed only weak influences of the vaned diffuser on the impeller flow field. This conclusion is partially substantiated by the successive vaned and vaneless diffuser tests described herein, in that, comparable impeller performances were obtained with either vaned and vaneless diffusers downstream.

Refinement of diffuser technology is continuing and could be assisted by the capability to operate sophisticated compressor test rigs with laser velocimeter equipment into, and beyond, the compressor surge or diffuser stall limitations to characterize the stall process and boundary layer behavior. This can be accomplished at lower rotational speeds without imminent mechanical complications. It is this zone that must be penetrated and stabilized if centrifugal compressor flow ranges are to be improved.

TEST RIG DESCRIPTION

The basic compressor rig depicted schematically in Figure 2 was used to calibrate over 29 different vaned diffusers. The rig was driven by a 500-horsepower direct current electric variable-speed motor driving through a speed increaser gearbox. The inlet airflow was measured with a bellmouth venturi, and subsequently ducted to the axial inlet guide vanes of the compressor. Airflow regulation was achieved with a butterfly valve at the discharge. The pressure and temperature at the compressor inlet and discharge were measured with Kiel probes and resistance temperature devices. Additional instrumentation included Kiel probes downstream of the inlet guide vanes, static pressure taps along the flowpath, automatic traverse capability with a cobra probe at 10 percent beyond the impeller tip diameter, and shroud pressure transducers. Overall compressor efficiency was determined by both temperature rise and input power measurements and included casing losses.

The mixed impeller exit vector conditions were computed using the insulated casing discharge total temperature, impeller tip static pressure, and the continuity equation assuming an impeller tip

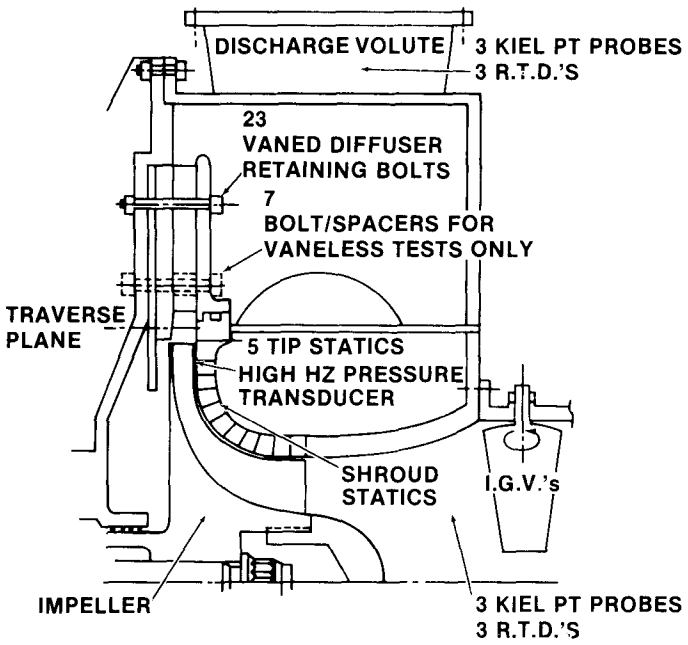

Fig. 2 Compressor test rig schematic

Downloaded from http://asmedigitalcollection.asme.org/GT/proceedings-pdf/GT1982/79566/V001T01A003/2394014/v001t01a003-82-gt-10.pdf by guest on 21 August 2022

blockage and recirculation plus windage correction according to Reference [2]. Impeller tip traversing, with a small cobra probe mounted on an electronically modulated traverse actuator, was conducted at several points along a selected constant speed line to determine impeller exit boundary layer displacement thickness and blockage. The axial inlet (zero camber) guide vanes were manually adjusted to permit calibrations at average inlet prewhirl angles of 0, +35, and -15 degrees. The impellers were tested at tip speeds between 600 and 1400 fps and were allowed to thermally stabilize in the insulated casing between all test points. Particular attention to thermal stability was observed with the low specific speed impeller stages.

Test Components and Diffuser Instrumentation

The test impeller geometries are described in References [1] and [2] and are all of the backswept, open-shrouded type specifically designed to encompass a large flow coefficient, or specific speed, range. Each impeller test was conducted with vaneless and vaned channel diffuser systems. At least two vaned diffuser configurations, usually of different throat area, were tested with each impeller.

Table 1 lists the basic geometric features of the vaned diffusers and Figure 3(a and b) compares the lowest and highest flow vane entry configurations. A typical vaned diffuser stage assembly is shown in Figure 4 prior to attaching the compressor rig front casing shroud.

The method of test analysis used to determine the impeller performance was similar to that in Reference [2], and was based upon stage enthalpy rise, flow continuity, and measured impeller tip static pressure. Diffuser performance was obtained

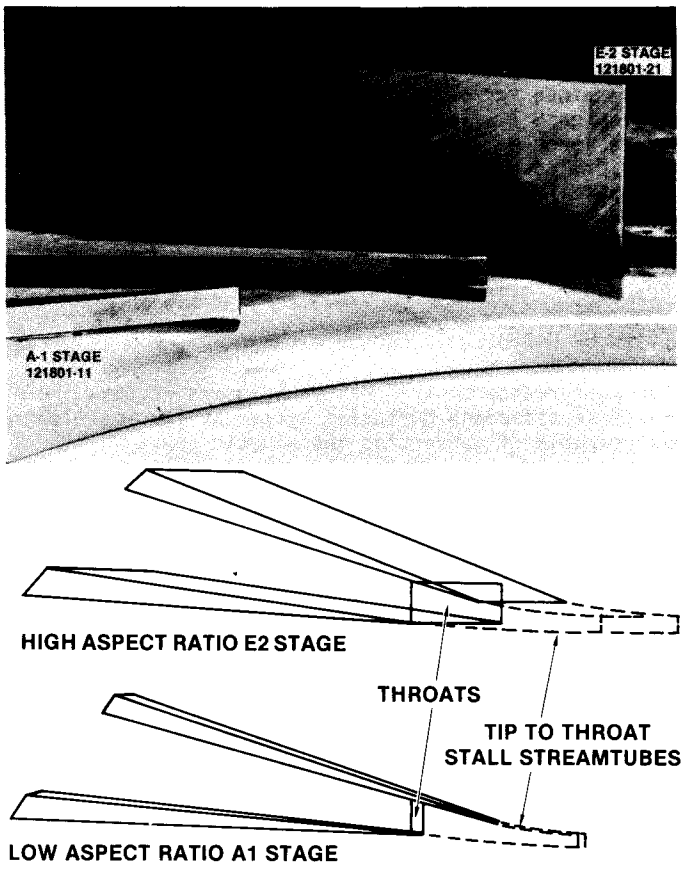

Fig. 3 Diffusers
(a) High aspect ratio
(b) Low aspect ratio

Table 1. Test Diffuser Geometries

Stage	$\frac{A_3}{}$ Sq. In.	$\frac{b_3}{D_3}$	$\frac{A_4}{A_3}$	$\frac{D_3}{D_2}$	Z	AS	$\frac{L}{W}$	$\frac{C_2}{C_3}$ Stall
D	22.8	0.078	2.17	1.18	21	0.72	6.4	1.8
D	22.8	0.082	2.03	1.13	13	1.0	5.0	1.5
D	22.8	0.081	2.03	1.14	21	0.96	6.4	1.8
C	22.0	0.069	2.1	1.14	21	1.15	5.2	1.75
C	17.0	0.065	2.36	1.21	21	1.5	6.2	1.85
A	6.5	0.031	2.59	1.13	21	0.77	6.2	1.8
A	6.5	0.031	2.32	1.13	13	0.48	5.0	1.28
E2	28.2	0.095	2.17	1.16	23	1.92	6.2	1.71
E2	33.8	0.101	1.98	1.09	23	1.6	5.2	1.51
E1	23.5	0.079	2.17	1.16	23	1.6	6.2	1.54
E1	28.2	0.084	1.98	1.09	23	1.32	5.2	1.5
D2	19.5	0.066	2.17	1.16	23	1.32	6.2	1.72
D2	23.4	0.069	1.98	1.09	23	1.1	5.2	1.6
D1	18.3	0.052	2.17	1.16	23	1.04	6.2	1.8
C2	9.7	0.039	2.40	1.21	23	1.03	9.4	1.4
C2	12.2	0.041	1.87	1.16	23	0.83	6.2	1.5
C1	9.7	0.039	2.4	1.21	23	1.03	9.4	1.5
C1	12.2	0.041	1.87	1.16	23	0.83	6.2	1.6
C1	9.7	0.042	2.4	1.12	23	1.03	9.4	1.5
B1	6.8	0.028	2.5	1.06	23	0.51	7.5	1.7
B1	5.7	0.026	2.75	1.12	23	0.68	10.0	1.40
A1	4.1	0.016	2.37	1.12	23	0.35	7.5	1.42
A1	3.4	0.017	2.51	1.06	23	0.41	10.0	1.26
A0	3.1	0.012	2.37	1.12	23	0.53	7.5	1.19
A0	2.6	0.013	2.75	1.16	23	0.32	10.0	1.27
Ref [1]	1.08	0.034	2.6	1.12	21	0.78	9.2	1.40

Downloaded from http://asmedigitalcollection.asme.org/GT/proceedings-pdf/GT1982/79566/V001T01A003/2394014/v001t01a003-82-gt-10.pdf by guest on 21 August 2022

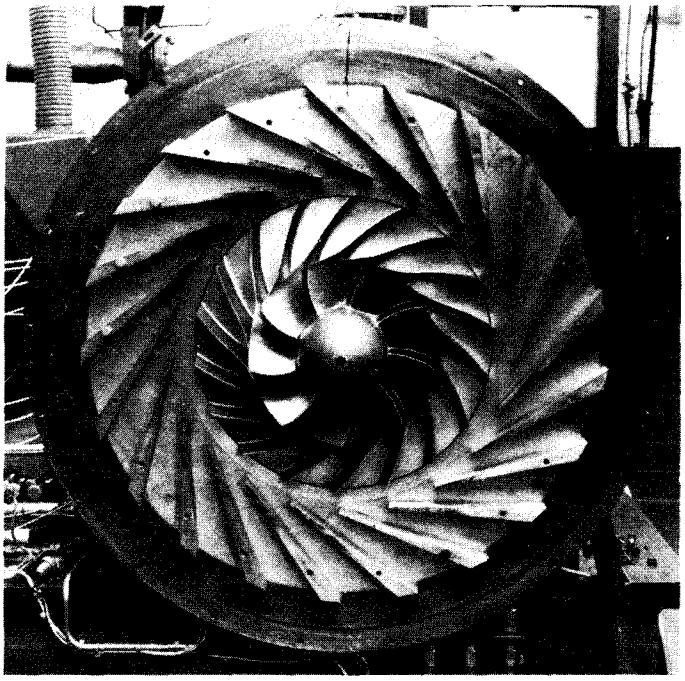

Fig. 4 Typical vaned diffuser test stage

from measured airflow and discharge temperature in conjunction with the following pressures:

- Channel diffuser throat static pressure
- Channel diffuser troat centerline stagnation pressure (See Figure 5)
- Channel diffuser exit static pressure

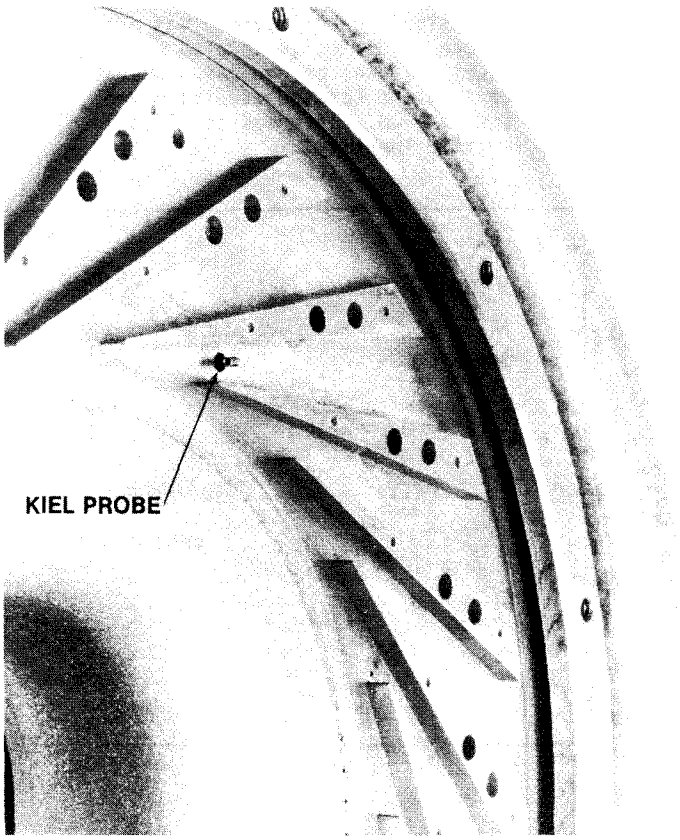

Fig. 5 Diffuser throat stagnation probe

Most of the data showed that the difference between the calculated impeller tip stagnation and diffuser throat centerline stagnation pressures were small (±0.5 psi) except in the vicinity of stage surge. This result may be more fortuitous than factual due to the selected housekeeping practices for impeller performance assessment, and inability to measure the mass averaged diffuser throat stagnation pressure. Fortuitous, or factual, the results are conceivable if mixing or recirculation losses are charged against the impeller, and if the "core flow" loss is small.

The significance of the impeller tip to diffuser throat pressure loss and its inherent difficulty in assessment, suggested an indirect diffuser performance parametric representation. Such a representation will be discussed after consideration of the inflow conditions entering the channel diffuser.

Impeller Exit Profile

Impeller tip traversing was conducted on several stages with a small cobra probe mounted at a diameter ratio of 1.1 in the vaneless space. Traverse data was obtained adjacent to impeller stall, at maximum (vaneless) stage efficiency, and near impeller choke along a selected constant speed line. Absolute flow angle and total pressure were measured with the probe. Flow profiles were calculated using these data together with the measured wall static pressure and discharge temperature.

A steady state data point was recorded to coincide with each impeller exit traverse. Typical normalized impeller meridional velocity profiles are shown on Figure 6 for four different impellers

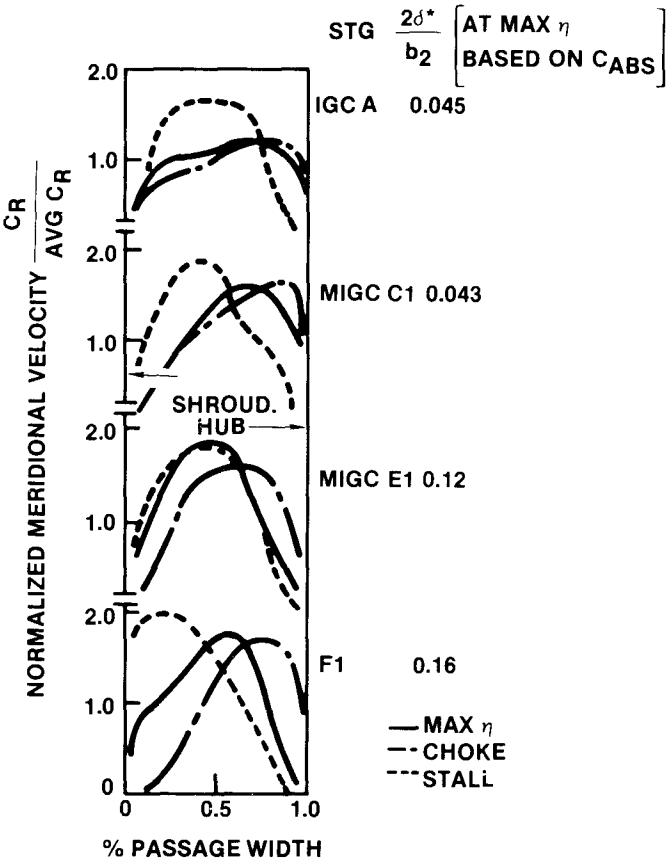

Fig. 6 Impeller exit flow profiles

Downloaded from http://asmedigitalcollection.asme.org/GT/proceedings-pdf/GT1982/79566/V001T01A003/2394014/v001t01a003-82-gt-10.pdf by guest on 21 August 2022

covering the low to high specific speed range. All exhibited well-developed profiles with a trend for shroud flow migration near surge, and hub flow migration near choke, particularly for the higher specific speed types. This is a consequence of the large shroud and hub curvatures intrinsic to high specific speed impellers.

Since diffuser performance is a function of inlet flow blockage, it was informative to calculate impeller tip blockage from the traverse data using the boundary displacement thickness of the absolute flow. Blockage factors varied from the order of 0.05 to 0.16 with increasing specific speed.

DIFFUSER PERFORMANCE

Compressor rig performance data were recorded with an automatic data acquisition system and subsequently reduced to vector conditions, efficiencies, and flow rates by computer techniques. Mapping was normally conducted at three speeds with several data points per speed line in addition to stall or surge. In some instances, performance of the impeller past stall toward the shutoff condition was recorded.

As will be discussed later, this stalled performance data proved to be particularly informative. For this analysis, the flow was studied between three stations: impeller tip, diffuser throat (vaneless space), and scroll exit.

The basic diffuser performance parameters calculated were:

Impeller Tip - Diffuser Throat Static Pressure Recovery

$$C_{p\ 2\text{-}3} = \frac{P_3 - P_2}{P_2 - p_2} \tag{1}$$

Diffuser Throat - Scroll Exit Static Pressure Recovery

$$C_{p\ 3\text{-}E} = \frac{P_E - P_3}{P_3 - p_3} \tag{2}$$

Diffuser Throat Blockage

$$B_3 = 1 - C_D \tag{3}$$

where

$$C_D = \frac{W}{\left(\frac{W\sqrt{T}}{\sqrt{AP}}\right)_3 \left(\frac{AP}{\sqrt{T}}\right)_3}$$

where

W = measured airflow

$\left(\frac{W\sqrt{T}}{AP}\right)_3 = Q_3$ flow function from $\left(\frac{P}{p}\right)_3$ measured

Pressure Loss Coefficient

$$\frac{P_2 - P_3}{P_2 - p_2} \tag{4}$$

Diffusion Ratio

$$\frac{C_2}{C_3} \quad \text{or} \quad \frac{C_2}{C_3^*} = \frac{C_2}{C_3}\ \frac{1}{C_D} \tag{5}$$

C_2: from impeller tip vector average conditions
C_3: from measured $(P/p)_3$
C_3^*: from Q_3 (using physical unblocked throat area)

The diffusion ratio C_2/C_3 was selected because of its relationship with $C_{p\ 2\text{-}3}$ and similarity to the impeller diffusion parameter of Reference [1].

In incompressible flow:

$$C_{p\ 2\text{-}3} = 1 - \left(\frac{C_3}{C_2}\right)^2 \tag{6}$$

For inviscid flow, the effect of Mach number (M_2) on $C_{p\ 2\text{-}3}$ for a given C_2/C_3 is relatively small as indicated in Figure 7. Examination of channel diffuser data in the practical range of interest (i.e., $C_{p\ 2\text{-}3} \geq 0$) showed that most of the test static pressure recoveries coalesced towards the inviscid identity relationship (This confirms the earlier statement that $P_2 \simeq P_3$.) Furthermore, diffusion ratios appeared to be limited to a maximum of 1.8. The notable exception is test data for the very low aspect ratio stage (A0) where increased friction losses are anticipated from the hydraulic analogy of the flow turning between the impeller tip and diffuser throat. (See Figure 3b.) Maximum diffusion ratios for the individual stages are listed in Table 1 and attain maximum values for the medium specific speed stages. Of significant interest was the monatomic increase of diffusion towards a maximum recovery at stall followed by decreased diffusion when operating into the stalled condition and furthermore the stalled recoveries still coalesced around the inviscid identity.

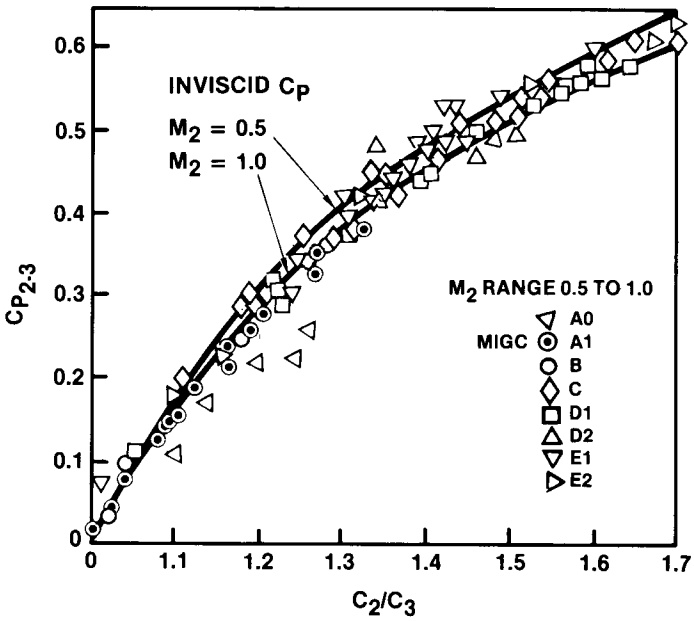

Fig. 7 Test recoveries $C_{p\ 2\text{-}3}$ versus C_2/C_3

Downloaded from http://asmedigitalcollection.asme.org/GT/proceedings-pdf/GT1982/79566/V001T01A003/2394014/v001t01a003-82-gt-10.pdf by guest on 21 August 2022

The maximum static pressure recovery in the vaneless space was on the order of 0.5 to 0.6 compared to an overall recovery between the impeller tip and exit of 0.7 to 0.8. Nearly three quarters of the impeller tip kinetic energy is recovered in this important region. The attainment of a limiting recovery became apparent upon examination of throat contraction factor C_D variation for stages operated up to, and past the peak stage pressure ratio.

Figure 8 shows such a result for an E1 stage where blockage increases gradually up to a maximum diffusion ratio of 1.55 followed by an inflexion and faster blockage growth with consequent reduced diffusion rates past stall. This suggested a primary reason for reduced static pressure recovery, and diffusion in stall may not be increased total pressure loss but rapid blockage growth.

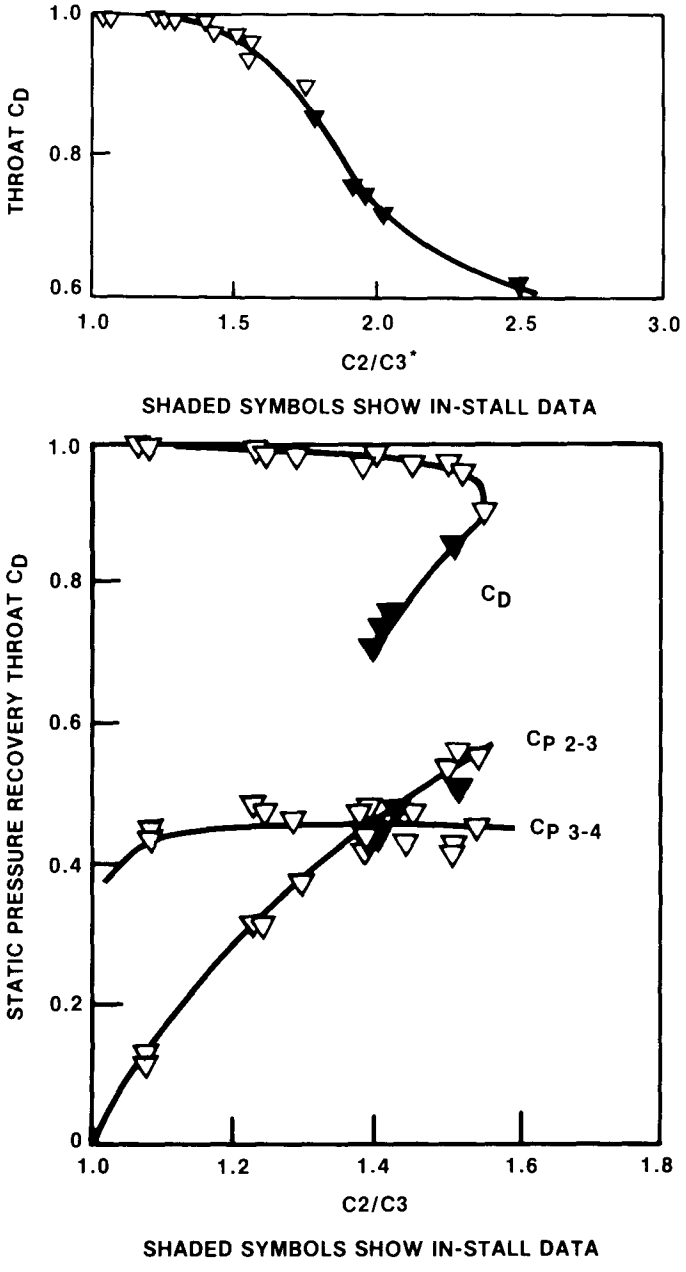

Fig. 8 Channel diffuser performance

Dual blockage factors for single diffusion ratios logically invoke correlation of blockage versus incidence as demonstrated by Kenny, Reference [8], for both conical pipe diffusers and centrifugal impellers. Incidence requires a definition of blade setting angle such as suction surface, mean, or equivalent throat angle. The large diffuser data base with aspect ratios ranging from 0.32 to 1.92, throat angles varying from 62 to 74 degrees, measurement uncertainties and repeatability, initially revealed an unsatisfactory incidence blockage correlation. Recognition of the throat geometries shown in Figure 3, potential blockage magnitude on the suction surface, and equivalent streamtube diffusion from the impeller tip to the diffuser throat, prompted examination of unblocked diffusion ratio, C_2/C_3, versus normalized blockage B_{3n} defined as:

$$\text{Normalized blockage } B_{3n} = \left[\frac{1-\left(\frac{C_D}{C_{D\ max}}\right)}{AS}\right] \quad (7)$$

(C_D max varied from the order of 0.9 to 1.1 under choked conditions)

Normalized blockage data for the test channel diffusers is shown on Figure 9 and indicates a large growth of blockage with increasing unblocked diffusion ratio C_2/C_3. (The concept of a critical blockage of 30 percent was established for axial compressor stages by Greitzer, Reference [10].) The mean trend is lower than that presented in Reference [8] for conical pipe diffusers, and substantiates comparative tests with both pipe and channel diffusers discussed in Reference [9]. At diffusion ratios C_2/C_3 = 2.2 (equivalent incidence of +10 degrees), the normalized throat blockage is shown to amount to one-third of the channel throat area.

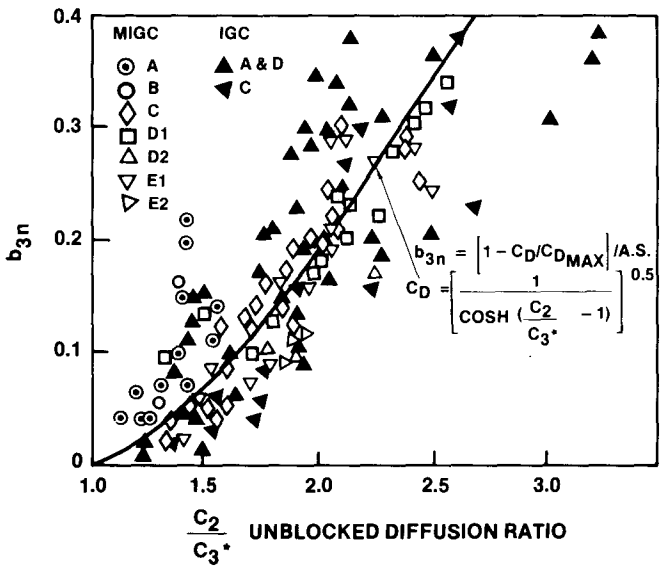

Fig. 9 Normalized blockage versus unblocked diffusion ratio

Downloaded from http://asmedigitalcollection.asme.org/GT/proceedings-pdf/GT1982/79566/V001T01A003/2394014/v001t01a003-82-gt-10.pdf by guest on 21 August 2022

The gross data manipulation leads to the following major observations for centrifugal compressor channel diffusers of the pertinent type with inlet Mach numbers from 0.4 and 0.8:

1. Diffusion or static pressure rise capability between the impeller tip and diffuser throat was limited to maximum velocity ratios C_2/C_3 on the order of 1.6 -1.8.

2. At large diffusion ratios, the throat blockage can amount to one-third of the physical throat area and severely impact the ensuing kinetic energy recovery causing a positive static pressure flow characteristic.

3. Static pressure recovery $C_{p\ 2\text{-}3}$, in and out of stall, coalesced toward the inviscid velocity ratio identity.

4. The influence of throat geometry and boundary layer accumulation on the suction surface in high aspect ratio diffusers represents a larger static pressure deficit.

5. The actual stall process is associated with $\partial^2 B_n/\partial(C_2/C_3)^2$ becoming zero.

The large data scatter for throat blockage variation is, however, substantial and could, in all probability, be coalesced further if the intimate end-wall hub and shroud blockage contributions were known (Reference [11]). The vaneless diffuser flow traverses, which were previously discussed, indicated that blockage growth in the vaneless space near the vaned diffuser throat (vaneless space diameter ratio 1.1) was from 5 to 16 percent.

Covered Channel Performance

The static pressure recovery of the covered channel from the physical throat to the channel (bounded exit for the various test diffusers are compared with the data of Reference [12] (inlet blockage = 0.05) on Figure 10. Test conditions and throat geometries, the covered channel area and length-to-width ratio approached the stalling limits as indicated by data points displaced towards the left. It was not possible to specifically isolate the effect of throat blockage on covered channel static pressure recovery.

The influence of covered channel diffusion capability on overall diffusion system recovery from the impeller tip to diffuser exit can be simply derived from the individual diffusion ratios, if incompressible inviscid flow is presumed in the vaneless space, as

$$C_{p\ 2\text{-}4} = \left[1 - \left(\frac{C_3}{C_2}\right)^2\right] + \left(\frac{C_3}{C_2}\right)^2 C_{p\ 3\text{-}4} \qquad (8)$$

This relationship is shown plotted in Figure 11 with representative limit ranges for the low Mach number [$M_2 \leq 0.8$] channel diffuser. Highest static pressure recoveries $C_{p\ 2\text{-}4}$ for the diffusers described herein were on the order of 0.88. Figure 11 illustrates the importance of both vaneless space and covered channel diffusion limitations. Note that, however, maximum performance potential (also flow range) is fundamentally determined by the diffusion ratio C_2/C_3. In length limiting diffuser installations, it is still also possible to obtain a respectable overall recovery level. This has been demonstrated with channel diffusers having only a small covered channel portion.

Experimental Investigations in the Vaneless Space

Although the premise that the viscous losses in the vaneless space are small elucidates blockage theory, losses arising from friction, mixing, and secondary sources are present. Flow turning between the impeller tip and throat in a low aspect ratio stream tube produces high losses. Alternatively, blockage friction with a high passage aspect ratio reduces static pressure recovery. Large vaneless space losses may appear in the vicinity of either impeller or diffuser stall, and can be accompanied by a sudden rise in impeller work factor (enthalpy rise). If this enthalpy is attributed to useful work

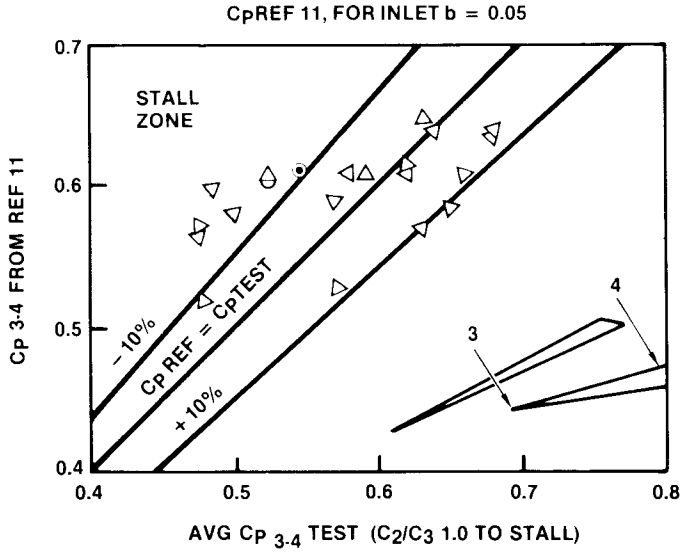

Fig. 10 Covered channel static pressure recovery

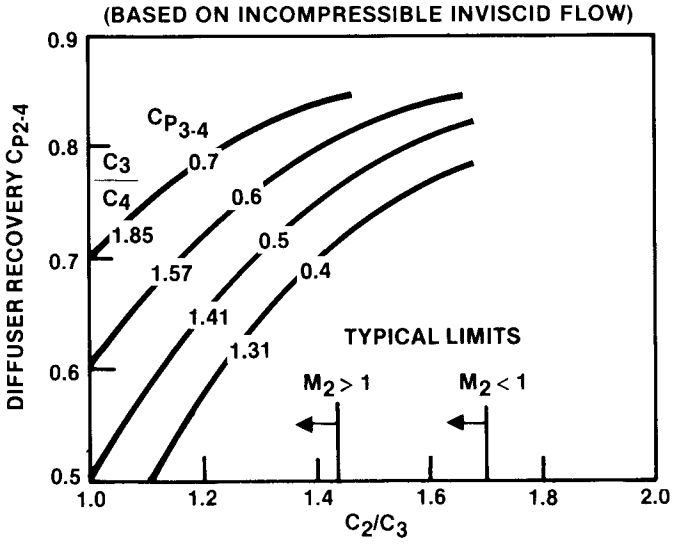

Fig. 11 Influence of vaneless space and covered channel recoveries on $C_{p\ 2\text{-}4}$

Downloaded from http://asmedigitalcollection.asme.org/GT/proceedings-pdf/GT1982/79566/V001T01A003/2394014/v001t01a003-82-gt-10.pdf by guest on 21 August 2022

by the impeller, the apparent vaneless space losses can be significant. In most instances, a rapid rise in work factor as flow is reduced beyond the peak stage efficiency and approaching stall is the result of flow recirculation from the vaneless space back into the impeller. A component performance analytical procedure, capable of recognizing this, would assist in diagnosis of the proper vaneless space losses. One approach can be to monitor impeller enthalpy rise and, at the occurrence of a noticeable increase near or in stall, charge the ensuing enthalpy increment to recirculation losses.

During analysis of this data, the largest vaneless space losses (up to one-third of local dynamic head) were noticed in some cases adjacent to and beyond stall and were indeed accompanied by a slight inflection in the impeller work factor versus flow characteristic. A distinction between vaneless space friction and recirculation losses was therefore impeded except in the special circumstance of the lowest specific speed stage with a diffuser throat aspect ratio of 0.32. For the time being, hydraulic friction analysis is probably the best approach for lower Mach number compressors where shock losses in the vaneless space are negligible. Since flow characterization in this region is difficult, dependence upon experimentation and empirical analysis of test data is the normal recourse.

Optimization of the vaneless space remains a controversial subject which dichotomizes designs into separate long or short spare philosophies. Practical experience with blade high cycle fatigue failures favors a design approach to at least a diameter ratio of 10 percent and preferably 15 percent. The results of extensive experimentation in the vaneless space region are highlighted as follows:

Effect of Mach Number

All stages listed in Table 1, with the exception of Reference [1] stage, were tested at impeller tip Mach numbers between 0.4 and 0.8 and were designed for industrial gas compressor applications. Development testing of small high pressure ratio centrifugal compressors for gas turbine application has also been conducted in parallel. The diffuser performance analysis used for the lower Mach number industrial stages was subsequently applied to the higher Mach number gas turbine compressor stages.

Diffuser performance data for Reference [1] impeller tested with a vaned diffuser is shown in Figure 12. Throat blockage is plotted versus unblocked diffusion ratio C_2/C_3 for test impeller tip Mach number (M_2) between 0.69 and 1.03. Surge limiting values of diffusion ratio C_2/C_3, and blockage and throat incidence are tabulated. Maximum diffusion ratio was essentially constant at C_2/C_3 = 1.4 along the surge line for the incident Mach number range. Note that the compressor stage was tested with inlet guide vanes providing impeller inlet prewhirl of both zero and 40 degrees (in the direction of rotation).

Small, high Mach number, centrifugal compressors are extremely sensitive to impact-type pressure probes placed in the vaneless space and diffuser. Therefore, most stage mapping is conducted excluding probe disturbing (particularly surge definition) effects. This limits assessment of surge diffusion ratios to the unblocked C_2/C_3 values.

SURGE DATA TABULATION

PREWHIRL DEG	MACH NO M2	b_{3n}	$\frac{C_2}{C_3}$	i_3 DEG
0	0.69	0.19	1.40	6.0
0	0.87	0.17	1.44	5.5
0	0.94	0.175	1.39	4.7
0	1.01	0.210	1.41	5.0
40	0.69	0.21	1.41	6.3
40	0.86	0.21	1.41	5.5
40	0.95	0.17	1.42	4.6
40	1.03	0.19	1.44	4.5

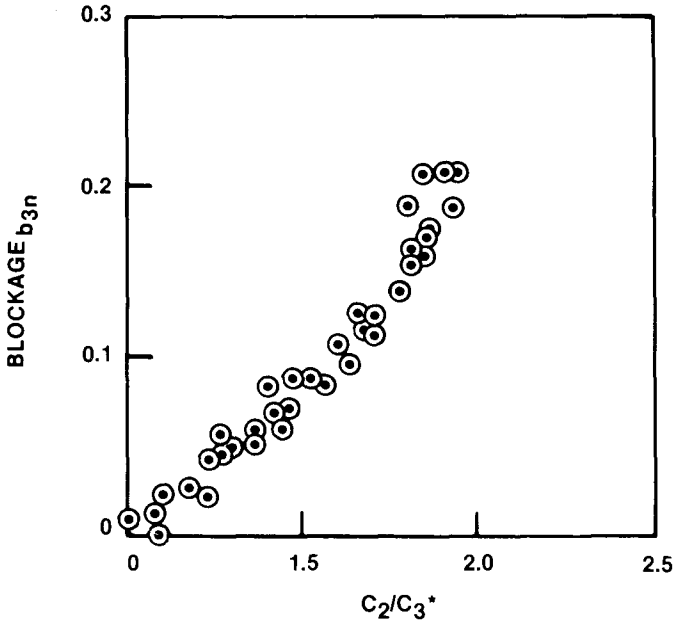

Fig. 12 Channel diffuser data Ref. 1 impeller

Representative unblocked diffusion ratios for higher Mach number stages tested are listed in Table 2 below.

Table 2. High Mach Number Diffuser Data

Impeller	Mach No, M_2	C_2/C_3	D_3/D_2
Ref. 1	1.02	1.76	1.125
HPRC	1.25	1.67	1.183
ARC2	1.16	1.40	1.166
MERDC	1.20	1.56	1.177

These unblocked diffusion ratios are lower and show a gradual reduction along each stage surge line as inlet Mach number is increased. This is not uncommon for high Mach number compressors, although a noticeable exception is the data in Reference [13].

Effect of Vaneless Space Diameter Ratio

The results of tests conducted on Reference [1] impeller with vaneless space ratios (diffuser leading edge/impeller tip) of 1.035, 1.125, 1.180, and 1.1215 are shown in Figure 13. The four tests were conducted with the same diffuser throat area in

Downloaded from http://asmedigitalcollection.asme.org/GT/proceedings-pdf/GT1982/79566/V001T01A003/2394014/v001t01a003-82-gt-10.pdf by guest on 21 August 2022

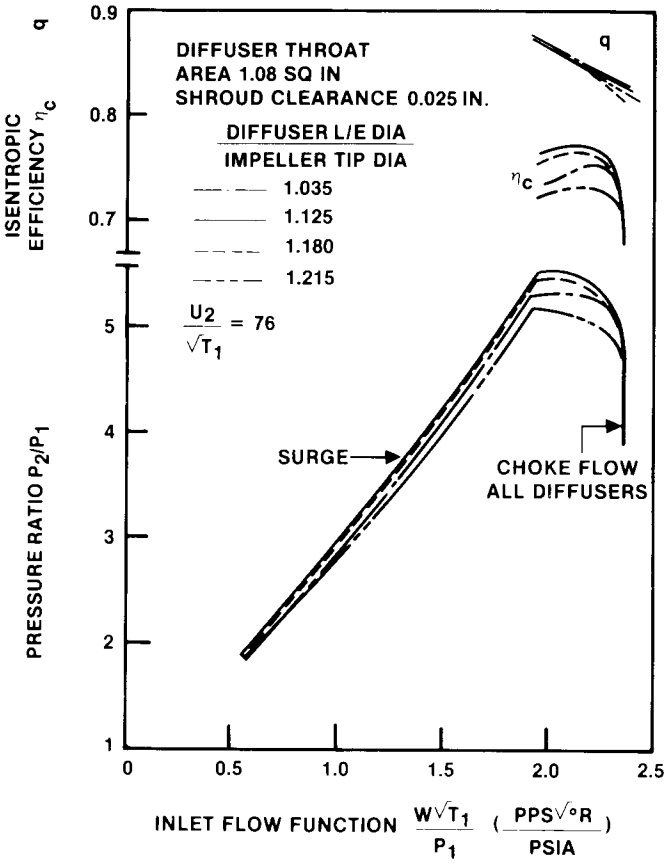

Fig. 13 Effect of vaneless space diameter ratio

order to preserve an optimum impeller/diffuser match and were accomplished successively by diffuser component removal only. For these particular compressor tests, maximum stage efficiency was obtained with a diameter ratio of 1.125. Note, however, that all four diffuser choke and stall flows at design speed were essentially equal, with the surge line displacement occurring as a result of delivery pressure differences. The impeller work factor was also essentially unchanged.

These specific test data indicate that diffuser flow range was not materially influenced by vaneless space diameter ratio, but diffuser losses apparently increased when the diameter ratio departed from the optimum value of 1.125.

Effect of Diffuser Vane Profile

The effect of diffuser vane profile on the performance of the radially bladed compressor with a pressure ratio of 4.0 is shown in Figure 14. Again, these particular tests were conducted with three diffusers of varying profile but constant throat area. All these diffusers choked at the same flow at 100 percent design speed, but surge characteristics and stage efficiency differences were observed. Maximum flow range and efficiency were achieved with a wedge, or vane island, contour having a straight suction surface.

Effect of Vane Number

Comparative performance tests of a high Mach number compressor with 41, 37 and 13 diffuser vanes of the same throat area are described in Reference [5]. No significant difference was obtained in compressor flow range with vane number variation. Similar tests have been conducted on several compressors with varying vane number at constant

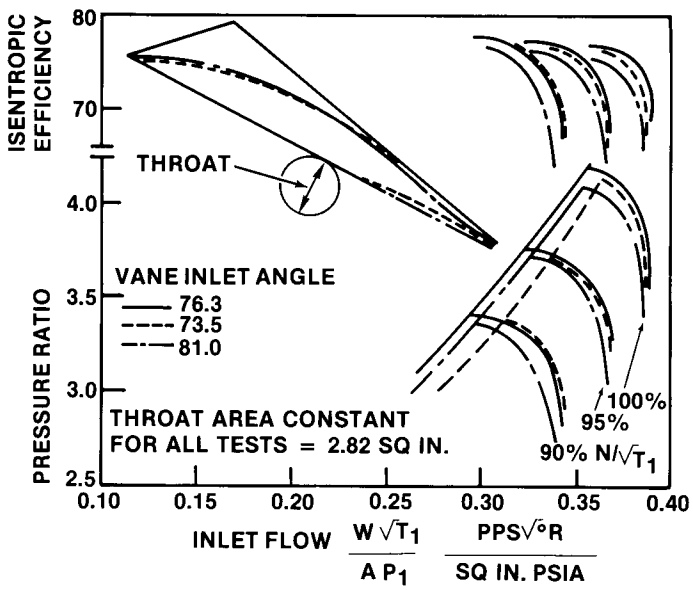

Fig. 14 Effect of diffuser vane profile

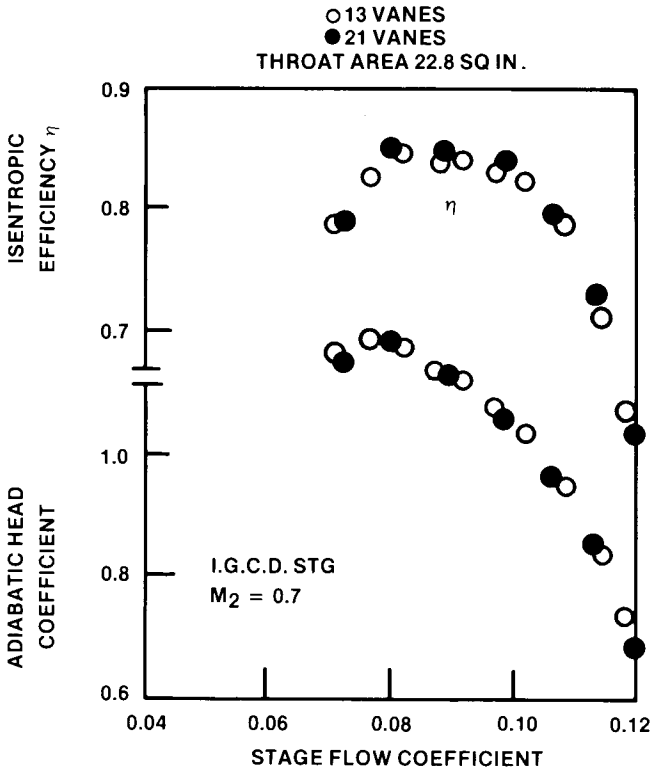

Fig. 15 Effect of diffuser vane number

throat area. In general, the changes in flow range, stall to choke, are minor yet, overall pressure recovery can change depending upon the covered passage performance. Minor changes in flow range and pressure recovery may increase overall system surge margin from unacceptable to permissible levels in surge sensitivity. Figure 15 shows a stage performance comparison of high efficiency, low pressure ratio stage (M_2 = 0.7) with both a 13 and 21 vane channel diffuser at the same throat area. Stage performance is virtually unchanged.

The effect of covered channel splitter vanes on the compressor in Reference [1] is shown in Figure 16. The splitters were designed not to penetrate the

Downloaded from http://asmedigitalcollection.asme.org/GT/proceedings-pdf/GT1982/79566/V001T01A003/2394014/v001t01a003-82-gt-10.pdf by guest on 21 August 2022

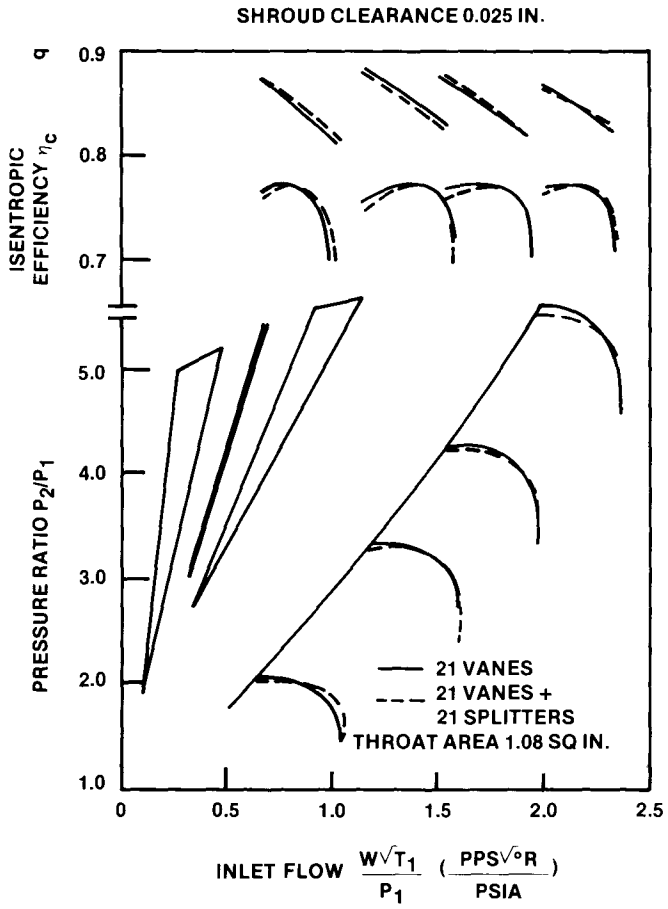

Fig. 16 Effect of diffuser splitters

diffuser throat, and were quite thin (0.023 inch). The compressor performance was unchanged. It would have been informative to follow this test with a covered channel of increased area ratio.

Effect of Diffuser Vane Suction Surface Bleed

The argument that the low momentum fluid accumulation on the suction surface may eventually precipitate surge suggested techniques for boundary layer suction prior to the diffuser throat. The relatively large thickness of the typical wedge diffuser permitted experimental test of the suction surface slot configuration shown in Figure 17. The slot opening was 0.011 inch (0.028 cm) and permitted approximately 2 percent of the inlet flow to be bled off upstream of the throat, which both increased flow range and stage efficiency in an instance where the stage characteristic was essentially dictated by diffuser stall and choke.

Effect of Impeller Back Shroud Bleed

The effect of impeller back shroud bleed extracted from the impeller tip on Reference [1] impeller is depicted in Figure 18. Bleeding of 4 percent of the inlet airflow resulted in an efficiency (based on temperature rise) improvement on the order of 4 percent. Net efficiency improvement, assuming the bleed flow could not be gainfully employed, would be zero.

Of special interest are the observations that the flow map was essentially displaced 4 percent with effectively a 4 percent larger diffuser throat restriction, and that peak pressure ratio remained

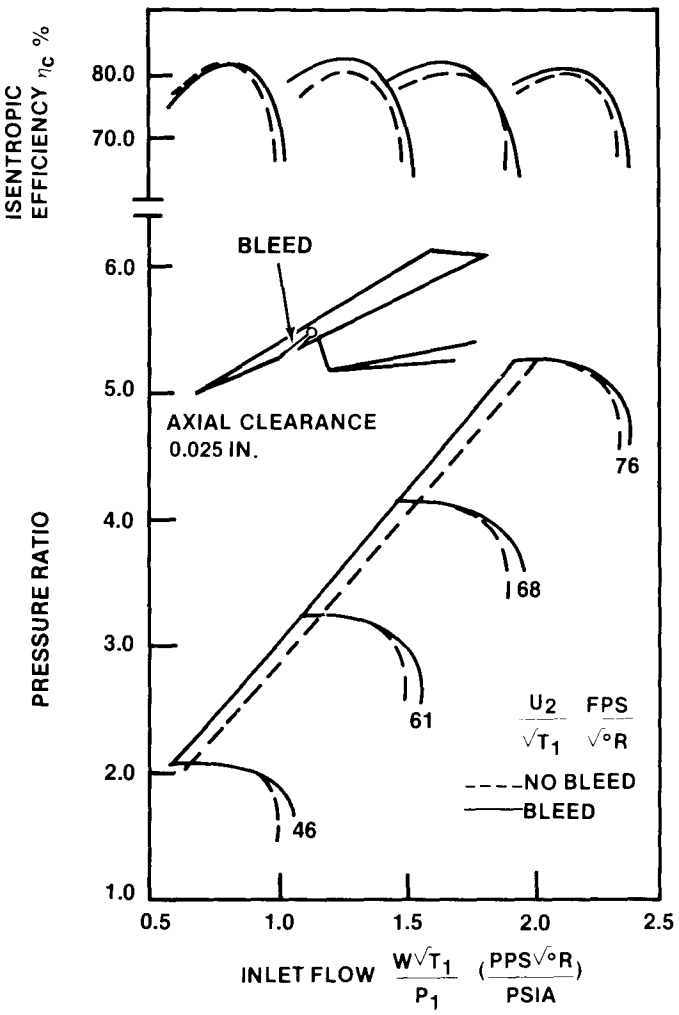

Fig. 17 Effect of suction surface bleed

unaltered, but work factor decreased approximately 4 percent. The efficiency improvement may, therefore, have resulted from a decrease in the recirculation flow between the diffuser and impeller tip and/or decreased back shroud windage losses.

Back shroud bleeding was subsequently tested on a more lightly loaded impeller with a work factor of 0.7, and no performance changes were observed. Recirculation could therefore be postulated to be more prone on highly loaded impellers with high absolute discharge flow angles.

Variable Diffuser Compressor Data

Various mechanical and aerodynamic methods of flow and pressure regulation through highspeed centrifugal compressors were discussed in Reference [14], together with the test data concerning the stage performance of a variable throat area diffuser compressor. Surge line data at the various throat settings for this particular compressor was re-analyzed using the C_2/C_3 correlation, and results are shown in Figure 19 a and b. With a diffuser vane end gap/height ratio of 0.9 percent surge C_2/C_3 for all four throat settings ranged from 1.35 to 1.70. As described in Reference [14], increasing the end gap ratio to 3.6 percent resulted in increased flow range, reflected by the shaded symbols shown in Figure 19(b).

Downloaded from http://asmedigitalcollection.asme.org/GT/proceedings-pdf/GT1982/79566/V001T01A003/2394014/v001t01a003-82-gt-10.pdf by guest on 21 August 2022

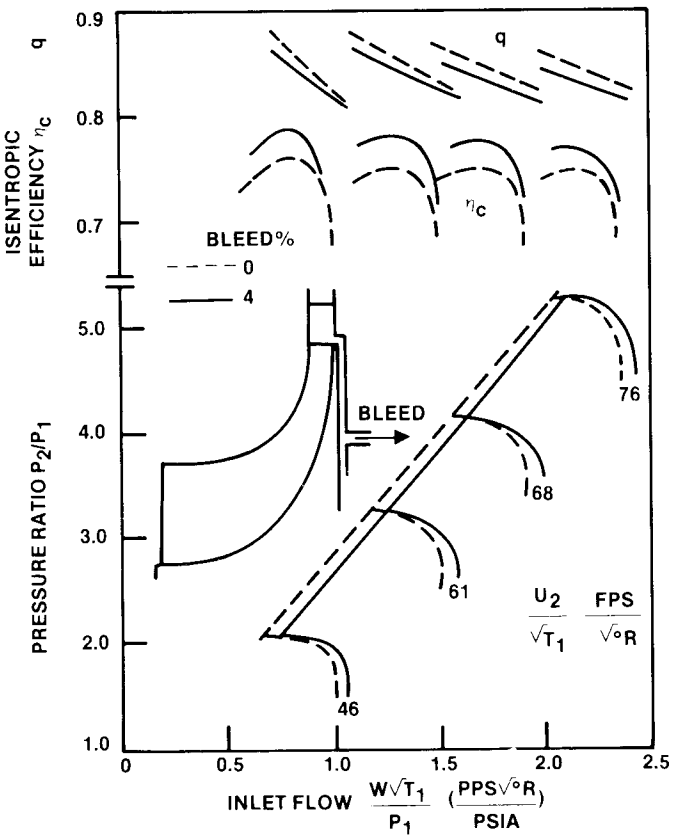

Fig. 18 Effect of impeller back shroud bleed

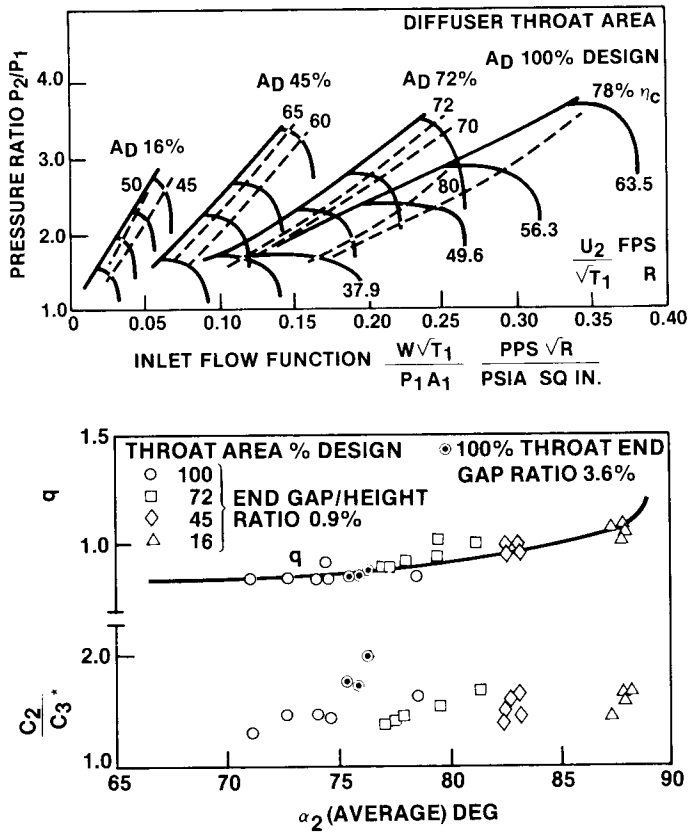

Fig. 19 Test data variable diffuser

These experimental test data related to the effect of vaneless space and covered channel conditions for certain centrifugal compressors are presented to illustrate the sensitivity of the vaneless space flow and the current inability of analytical treatment to predict its flow characteristics. The results are not repetitive from machine to machine as demonstrated by the described back shroud bleed experiments. They are, however, informative and deserve use for reference purposes.

CONCLUSIONS

Test data from numerous single-stage centrifugal compressors with channel diffusers was used to obtain a correlation of diffuser stall versus a limiting diffusion ratio between the impeller tip and diffuser throat. For any given stage, it was determined that stage surge (when triggered by diffuser stall) occurred near a constant tip-to-throat diffusion ratio, except as the impeller tip Mach number exceeded unity, in which case diffusion capability diminished. The diffusion ratio C_2/C_3 attained a maximum value on the order of 1.8, but was not unique for all stages being more intimately coupled with throat blockage accumulation as a function of diffusion rate. Near the limiting diffusion ratio, the throat blockage could amount to one-third of the physical throat area, and operation into stall revealed continuing blockage accumulation with reducing throat static pressure rise. The stall process for centrifugal compressor stages with vaned diffuser thus appears to be similar to that of axial compressor stages in that a critical blockage (Reference [10]) is reached. Large data scatter for normalized throat blockage versus diffusion ratio was experienced when comparing all stages. The general trend indicated that the actual stall process may be associated with:

$$\frac{\partial^2 B_n}{\partial (C_2/C_3)^2} \rightarrow 0 \qquad (9)$$

Most of the static pressure recovery test data measured between the impeller tip and the diffuser throat coalesced towards the inviscid velocity ratio identity, both approaching, entering, and operating in stall. This would imply that, for this particular analysis, the core flow total pressure loss was small. An exception was test data for the very low aspect ratio diffusers where increased friction losses are anticipated from the hydraulic analogy of the flowpath.

The influence of throat geometry and boundary layer accumulation on the suction surface in higher aspect ratio diffusers represents a potentially larger static pressure deficit. Throat aspect ratios of around unity are therefore expected to produce optimum diffuser performance.

Insufficient instrumentation in the covered section of the diffuser channel prevented a better analysis of the influence of throat blockage on C_{p3-4}. A comparison with two-dimensional diffuser data indicated reasonable agreement except in instances where the covered channel was operating near or in the stall condition.

Long covered channels can improve stage static pressure recovery, but maximum diffuser overall performance, in terms of flow range and static

Downloaded from http://asmedigitalcollection.asme.org/GT/proceedings-pdf/GT1982/79566/V001T01A003/2394014/v001t01a003-82-gt-10.pdf by guest on 21 August 2022

pressure, is more fundamentally determined by the vaneless space diffusion ratio C_2/C_3. Thus, even in length limiting diffuser installations, it is possible to obtain a respectable overall diffuser static pressure recovery level.

The justification for using a mean stream diffusion ratio approach in such a complex flow pass, dominated by endwall and flow mixing effects, comes primarily from convenience. The intent was to derive a simplified stall parameter that could be used in the preliminary design phase prior to detailed internal flow analysis. More sophisticated fluid dynamic models capable of predicting boundary layer growth, corresponding viscous shear and mixing losses, and separation onset in highly unsteady-flow may eventually be derived for vaneless space flow characterization. For the immediate future, more experimentation as typified by the extensive work described herein is prescribed: hopefully, with improved instrumentation techniques.

The experimental work necessary to provide an improved understanding should encompass investigating several flow stages from low to high specific speed operating both in and out of the surge or stalling zones.

ACKNOWLEDGEMENT

The author wishes to acknowledge the efforts of R. Geiser, Senior Development Engineer who assisted in the computer analysis of the test data.

REFERENCES

1 Rodgers, C., "Impeller Stalling as Influenced by Diffusion Limitations," ASME Journal of Fluid Mechanics , March 1977

2 Rodgers, C., "A Diffusion Factor Correlation for Centrifugal Impeller Stalling," ASME 78-GT-61

3 Blair, L.W., and Russo, C.J., "Compact Diffuser for Centrifugal Compressors," A.1.A.A. -80-1077

4 Rundstadler, P.W., Jr. and Dean, R.C., Jr., "Straight Channel Diffuser Performance at High Inlet Mach Numbers," ASME Journal on Basic Engineering , Vol. 91, No. 3 September 1969

5 Came, P.M., Herbert, M.V., "Design and Experimental Performance of Some High Pressure Ratio Centrifugal Compressors," AGARD -CP-282, 1980

6 Yoshinaga, Y., Gyobu, I., Mishina, H., Koseki, F., Nishida, H., "Aerodynamics Performance of a Centrifugal Compressor with Vaned Diffusers," ASME Journal of Fluids Engineering , December 1980

7 Krain, H., "A Study of Centrifugal Impeller and Diffuser Flow," ASME 81-GT-9

8 Kenny, D.P., "A Novel Correlation of Centrifugal Compressor Performance of Off-Design Prediction," A.1.A.A. -79-1159

9 Rodgers, C. and Sapiro, L., "Design Considerations for High Pressure Ratio Centrifugal Compressors," ASME 72-GT-91

10 Greitzer, E.M., "Review of Axial Compressor Stall Phenomena," ASME Journal of Fluids Engineering , June 1980

11 Conrad, O., Raif, K., Wessels, M., "The Calculation of Performance Maps for Centrifugal Compressors with Vane-Island Diffusers," Performance Prediction of Centrifugal Pumps and Compressors , ASME 1980

12 Reneau, L.R., Johnston, J.P., and Kline, S.J., "Performance and Design of Two Dimensional Diffusers," ASME Journal of Basic Engineering , Vol. 89, March 1967

13 Japikse, D., "The Influence of Diffuser Inlet Pressure Fields on the Range and Durability of Centrifugal Compressor Stages," AGARD -CP-282, 1980

14 Rodgers, C., "Variable Geometry Gas Turbine Radial Compressors," ASME 68-GT-63

Downloaded from http://asmedigitalcollection.asme.org/GT/proceedings-pdf/GT1982/79566/V001T01A003/2394014/v001t01a003-82-gt-10.pdf by guest on 21 August 2022